



Mapping molecular dynamics (Na_2) in intense laser fields: another dimension to femtochemistry

T. Frohnmeyer^a, M. Hofmann^a, M. Strehle^a, T. Baumert^{b,*}

^a *Physikalisches Institut, Universität Würzburg, 97074 Würzburg, Germany*

^b *Fachbereich Physik, Universität Kassel, Heinrich Plett Strasse 40, 34132 Kassel, Germany*

Received 28 July 1999

Abstract

Time-resolved photoelectron spectroscopy in combination with femtosecond pump–probe and molecular beam techniques is used to map the vibrational wavepacket motion along the internuclear coordinate. Using an attenuated femtosecond pump pulse and a probe pulse with variable intensity, the influence of high laser fields on the molecular potential is detected sensitive to the internuclear distance. We observe electronic transitions at non-Franck–Condon allowed areas which are attributed to light-induced potentials. © 1999 Elsevier Science B.V. All rights reserved.

1. Introduction

Besides femtochemistry where ultrashort laser pulses are used to monitor and control molecular dynamics in real time (see, e.g., Refs. [1–3]) the interaction of intense ultrashort laser pulses with atoms and molecules is a current research topic in the area of gas-phase ultrashort phenomena. This is because the intense electric fields available in femtosecond laser pulses exceed those of the binding of the outer-shell electrons in atoms and molecules as well as the field of the internuclear binding in molecules. These intense laser fields offer the possibility to investigate fundamental effects such as molecular-bond softening and above-threshold ionization (ATI) and above-threshold dissociation (ATD)

where the atoms or molecules absorb more photons than necessary to ionize or dissociate. Of practical interest is high harmonic generation and the possibility of X-ray lasers as a table-top source of short wavelengths.

The interaction of diatomic molecules with intense laser fields has been extensively studied in the last 10 years. In I_2 and N_2 Coulomb explosion and tunneling are demonstrated [4]. To explain the photoelectron spectra of N_2 and H_2 , Rydberg states being Stark shifted in resonance have been invoked [5]. These effects of intense laser fields depend on the internuclear distance as demonstrated in highly charged molecular ions of I_2 [6,7]. The results could be explained by a nonadiabatic electron localization field. The trapped population in this light-induced potential is able to tunnel through the internal Coulomb barrier of the diatomic molecule into the continuum [8]. Hence the rate of non-linear ioniza-

* Corresponding author. Fax: +49-561-804-4453; e-mail: baumert@physik.uni-kassel.de

tion in strong laser fields depends sensitive on the molecular configuration and provides a probe of molecular structure and motion.

Evidence of trapped population in light-induced vibrational states was found in ATD measurements in H_2^+ and D_2^+ [9] and explained in terms of a dressed-state potential, where the shape of the potential is due to the interaction of the ionic electronic state with the intense laser pulse. A theoretical extension of this picture examines quantum wavepacket propagation in intense laser fields for the Na_2^+ case [10]. It is demonstrated that the laser pulse duration can be used as a control parameter for both the dissociation probability and the branching ratio between different dissociation channels. To investigate this effect experimentally, the pulse duration must be shorter than the vibrational period of the molecule. From an experimental point of view, this is why these kinds of experiments are performed more easily on alkali dimers [11–13] with a typical oscillation period of roughly 300 fs as compared to the H_2 molecule with an oscillation period of about 15 fs. In a recent single-pulse experiment, different dissociation channels in Na_2^+ have been investigated, where the ultrashort intense laser pulse interacted with Na_2^+ molecules prepared in a well-defined vibrational state [14].

The scope of the experiment presented here is to study effects of intense laser fields sensitive to the internuclear distance in a neutral diatomic molecule. The following strategy has been implemented experimentally. We prepare well-defined vibrational wavepackets on the electronic states of Na_2 with an attenuated pump pulse [15]. After the pump-pulse interaction, the wavepackets move in unperturbed electronic potentials. A time-delayed ultrashort laser pulse of variable intensity is used to induce a high laser field interaction at a specific internuclear distance. The vibrational wavepacket evolution over the entire energetically allowed distance is mapped via photoelectron spectroscopy [11]. In general kinetic photoelectron spectroscopy in combination with femtosecond pump–probe technique has proven to be a powerful tool for probing the electronic and dynamical properties of molecular systems [11,16–20].

In the experiments described in this Letter, we observe electronic transitions in non-Franck–Condon allowed areas by increasing the intensity of the probe

laser. This observation is attributed to the effect of light-induced dressed-state potentials.

2. Experimental

The general experimental setup is described in detail elsewhere [21] and will be summarized briefly in the following. The femtosecond laser pulses are provided by a home-built Ti:Sapphire oscillator with a chirped pulse amplification (CPA) system. These pulses of 800 nm (90 fs, 1 mJ, 1 kHz) are frequency-converted into pulses of 620 nm at 20 μJ and 70 fs employing an optical parametric generator (OPG) including a subsequent prism compressor. In a Michelson-type setup, the beam is split into two equal parts and a variable time delay is introduced. Both beams can be attenuated separately to adjust the intensity of the pump and probe laser. The recombined laser beams are focused with a 300 mm lens into the vacuum chamber where the laser interacts with the molecular beam. Attenuated laser intensities ranging from 10^{11} to 10^{12} W/cm^2 are used in this experiment.

The sodium dimer is prepared vibrationally cold by supersonic expansion of sodium from an oven operated at 900 K through a nozzle of 200 μm diameter orifice into a differentially pumped vacuum chamber. The Na_2 beam is skimmed and directed through the pole-pieces of a magnetic bottle electron spectrometer [22] (MBES, Applied Laser Technology) where it intersects the laser beam perpendicular. The photoelectron spectra are recorded by their time-of-flight (TOF) distribution in the MBES using a 1 GHz, 2 gigasample digital oscilloscope and averaged over several thousands of laser shots. The energy resolution is 30 meV for electrons with a kinetic energy of 0.7–1.0 eV. Because of the high efficiency in electron collection of a MBES it is possible to perform the measurements at low densities of Na_2 in the interaction region. This is crucial in order to minimize space-charge effects in strong laser fields. In addition, a linear TOF-mass spectrometer is used to detect the corresponding ions. This enables us to compare the excitation conditions in the photoelectron experiment to the well-studied multiphoton ionization dynamics of Na_2 (at 2 eV photon energy excitation) [12,15].

The excitation scheme of the experiment is depicted in Fig. 1 including only the relevant molecular potentials (for detailed discussion, see Refs. [12,15]). The laser excitation centered at 620 nm couples the

neutral ground-state $X^1\Sigma_g^+$ to the ionic ground-state $X^2\Sigma_g^+$ via two resonant neutral states. Due to the Franck–Condon principle, and due to the spectral width of the 70 fs laser pulse, a one-photon transition

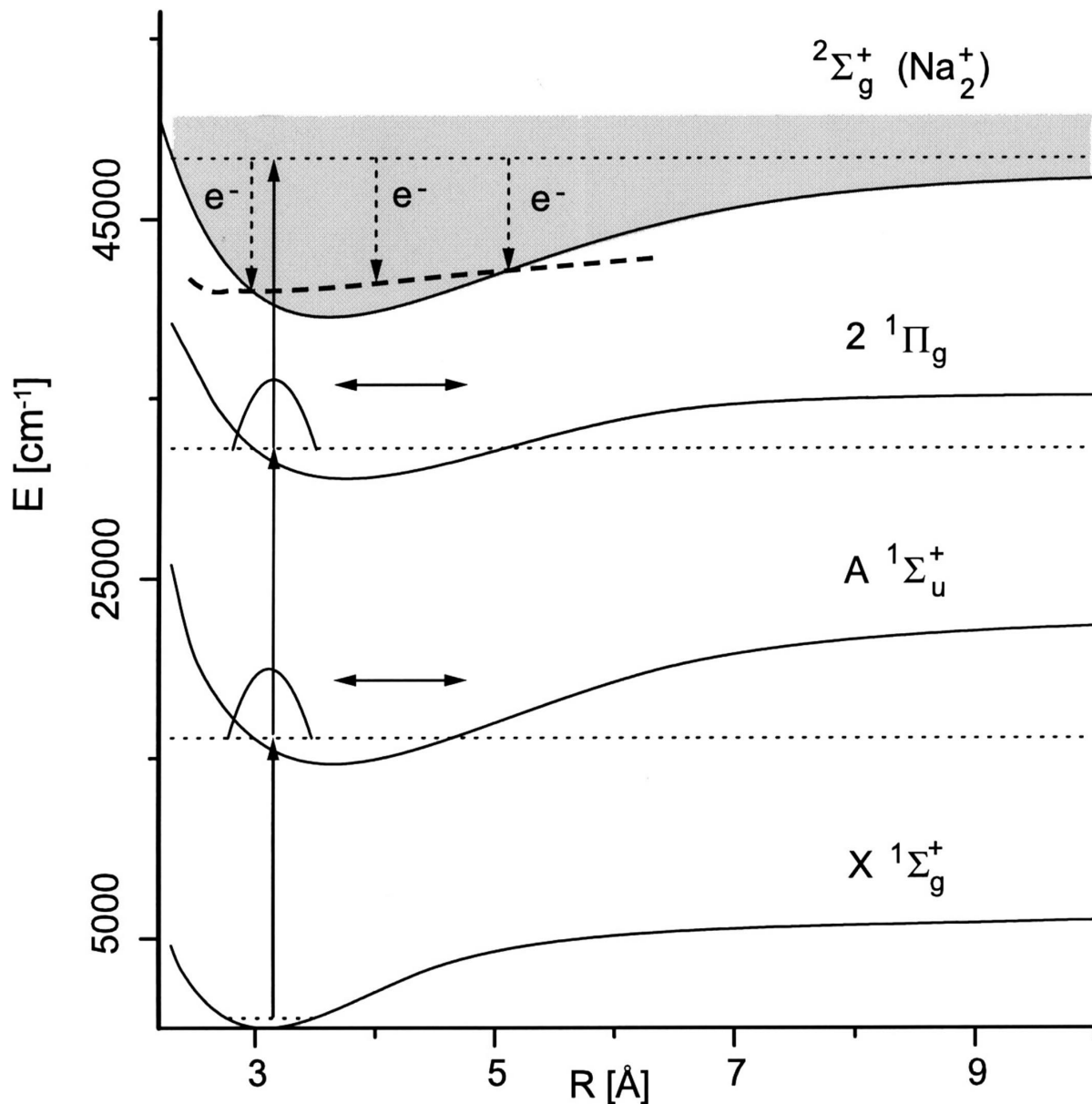


Fig. 1. Unperturbed potentials of Na_2 . The pump laser at 620 nm creates wavepackets in the $A^1\Sigma_u^+$ - and $2^1\Pi_g$ -states at the inner turning points. The time-delayed probe laser ionizes the sodium dimer. As indicated, the kinetic energy of the photoelectrons depends on the internuclear coordinate because of the monotonously increasing difference potential $(X^2\Sigma_g^+(\text{Na}_2) - 2^1\Pi_g + 2\hbar\omega)$, dashed line). The kinetic energy of the photoelectrons ranges from 0.93 to 0.8 eV for electrons created at the inner and outer turning point, respectively.

creates a wavepacket at the inner turning point of the $A^1\Sigma_u^+$ -state by coherent superposition of vibrational levels centered around $\nu' = 12$ –13 (in the following denoted as A-wavepacket). Additionally a wavepacket is prepared at the inner turning point of the $2^1\Pi_g$ -state centered at vibrational levels of $\nu' = 16$ –18 (Π -wavepacket) by absorption of two photons of the pump laser resonance enhanced by the $A^1\Sigma_u^+$ -state. After the excitation, the wavepackets propagate in unperturbed potentials with roundtrip times of about 310 fs ($\approx 110 \text{ cm}^{-1}$) and 370 fs ($\approx 90 \text{ cm}^{-1}$) in the $A^1\Sigma_u^+$ - and $2^1\Pi_g$ -states, respectively.

The propagation of the wavepackets is monitored by the time-delayed probe laser pulse which ionizes the molecules. The kinetic energy of the electrons created in a direct ionization process out of the $2^1\Pi_g$ -state is given by the difference potentials between the ionic ground state and the neutral Π -state ($X^2\Sigma_g^+(\text{Na}^+) - 2^1\Pi_g + 2\omega$) [11,23,24]. The difference potential of these molecular states is displayed

in Fig. 1 as a dashed line. Since this potential increases monotonously with the internuclear distance, it is possible to attribute the kinetic energy of the electrons to an internuclear distance. Electrons created at the inner turning point are formed with an energy of 0.93 eV whereas photoelectrons created at the outer turning point hold an kinetic energy of 0.8 eV.

3. Results and analysis

In Fig. 2a, the measured TOF photoelectron distribution is shown as a function of the pump–probe delay for the same intensity $I_0 \approx 10^{11} \text{ W/cm}^2$ of pump and probe laser. The TOF range from 0.8 to 1.15 μs displayed in the figure corresponds to a kinetic energy of the electrons from 1.1 to 0.6 eV. By varying the pump–probe delay, the dynamics of the sodium dimer in the two neutral states ($2^1\Pi_g$ and $A^1\Sigma_u^+$ via the $2^1\Pi_g$) is monitored. Particularly

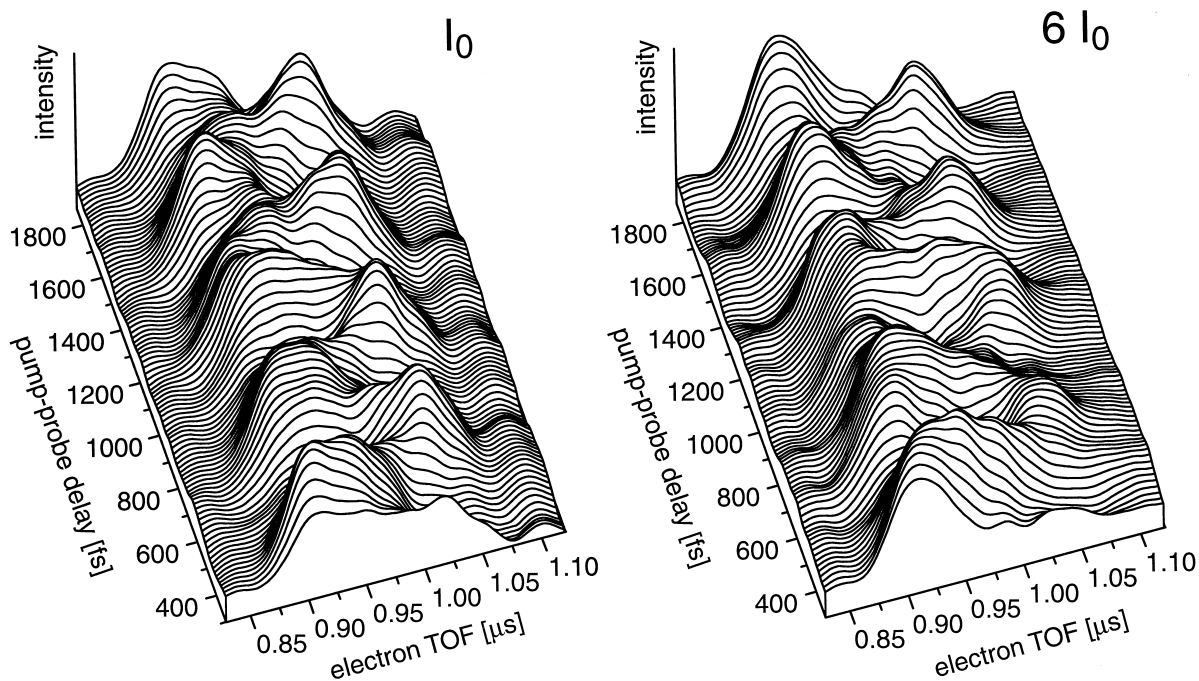


Fig. 2. (a) TOF photoelectron distribution as a function of pump–probe delay for attenuated pump and probe lasers at an intensity of $I_0 \approx 10^{11} \text{ W/cm}^2$. The dynamic of the wavepackets is monitored on an internuclear coordinate from about 3–5 Å. (b) Photoelectron distribution for the same pump laser intensity but a probe intensity of $6 \cdot I_0$. The dynamic behavior has changed but still the wavepackets can be clearly resolved.

the propagation of the $2^1\Pi_g$ wavepacket between the turning points is resolved. Since these points are attributed to an internuclear distance of 3–5 Å, by the difference potential analysis the vibrational dynamics of the sodium dimer is resolved in sub-Ångström resolution.

In order to deduce more dynamical information, we performed a fast Fourier transformation (FFT) along the pump–probe delay at 0.9 and 1.02 μs time of flight, corresponding to the inner and outer turning point of the wavepackets in the $2^1\Pi_g$ -state (Fig. 3, top).

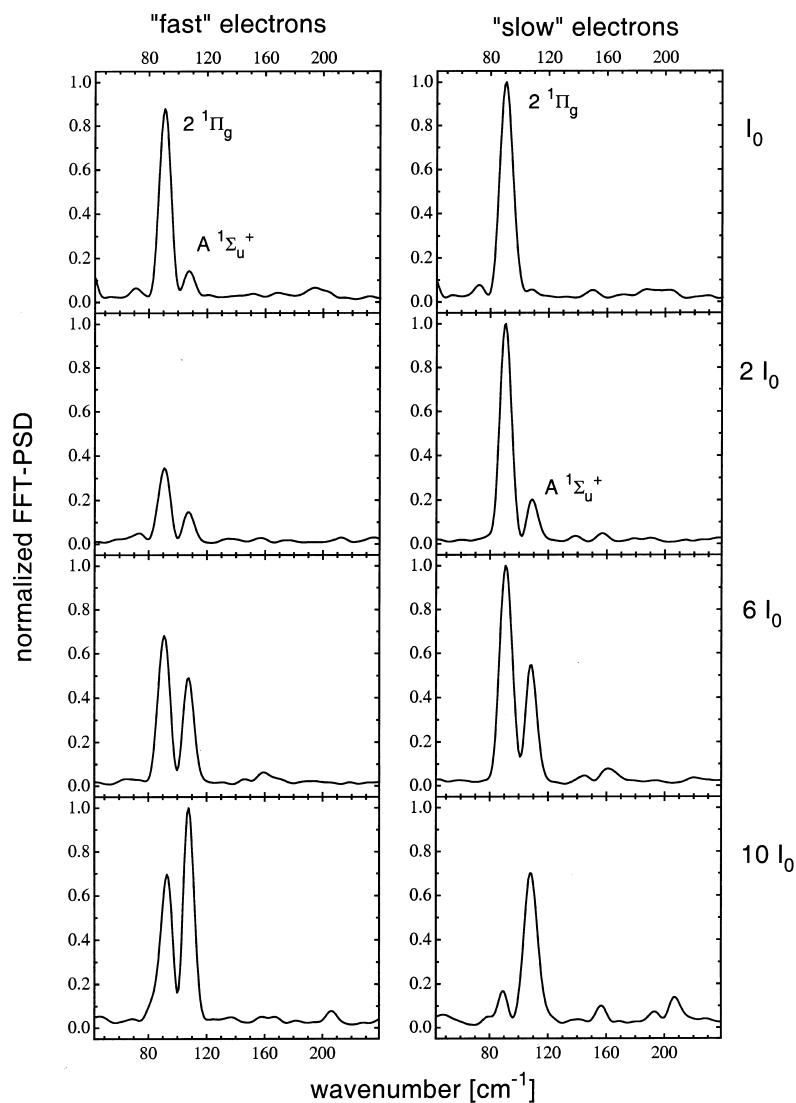


Fig. 3. Cuts of the normalized FFT spectra at two fixed TOF, representing the inner (left, 0.90 μs) and outer (right, 1.02 μs) turning point of the wavepackets. By increasing the probe laser intensity, the contribution of the A-wavepacket for the 'fast' photoelectrons increases in relation to the Π -wavepacket. For 'slow' photoelectrons, the contribution of the A-wavepacket starts to appear at intermediate intensities and increases fast with increasing laser intensity. This behavior is attributed to the effect of perturbed molecular potentials in high laser fields (dressed states). The minor frequency contributions are attributed to ground-state contribution and harmonics of the A- and Π -wavepacket.

There are two dominant contributions to the whole dynamics in the Fourier spectrum at about 90 and 110 cm^{-1} originating from the wavepackets in the Π - and A-state, respectively. At the inner turning point, we observe both contributions whereas, at the outer turning point, there is just the signal at 90 cm^{-1} . This can be explained in terms of the difference potential picture of the A- and Π -states depicted in Fig. 4 and also discussed in Refs. [15,23]. With attenuated laser intensities, a resonance-enhanced ionization out of the A-state via the Π -state is allowed at internuclear distances, where the difference potential equals the photon energy. Therefore, in the sodium dimer, there is a Franck–Condon window in the transition probability limited to the region of the inner turning point of the wavepacket propagation in the A-state. As a consequence, we observe a resonance-enhanced transition at the inner turning point of the wavepacket in the A-state but none at its outer turning point. The wavepacket propagation in the Π -state can be observed at all allowed internuclear distances since in this direct ionization process there is no limitation to a specific internuclear distance.

The population of the $A^1\Sigma_u^+$ - and $2^1\Pi_g$ -states induced by the pump laser depends on the pump laser intensity. Even at the low pump intensity used, coherent population transfer in Rabi-like oscillations affect the initial population in these intermediate

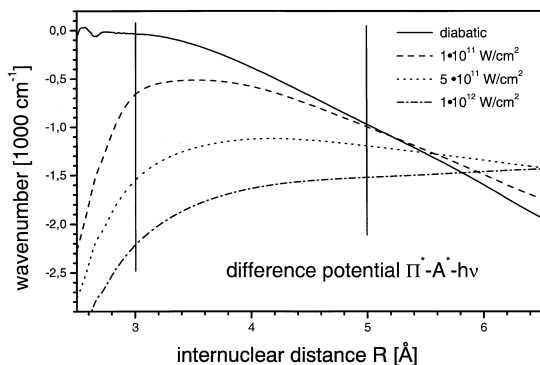


Fig. 4. Difference potential calculated in an adiabatic picture for different laser intensities. In the diabatic limit, the difference potential $\Pi^* - A^* - \hbar\omega$ equals the photon energy at small internuclear distances R and decreases with increasing R (solid line). At an intensity of $5 \times 10^{11} \text{ W/cm}^2$ the potential is almost flat in the relevant region of R (dotted line).

states [12,25]. This was verified by comparing the transient ion mass spectra of Na_2^+ , recorded at excitation conditions identical to those in the electron measurements with transient ion mass spectra published in Ref. [12]. As a consequence, the signal height in the FFT corresponding to the dynamics in a specific intermediate state depends on the pump laser intensity. This effect can be used to alter the initial population of the intermediate states in the pump–probe experiment since the propagation of the wavepackets after the pump excitation evolves in unperturbed potentials. In the experiments described in this Letter, we adjusted the pump laser intensity to detect both wavepackets in the intermediate states.

In a set of measurements, the pump laser intensity is kept fixed whereas the probe laser intensity is increased from $I_0 \approx 10^{11} \text{ W/cm}^2$ to $10 \cdot I_0$. As the excitation of the wavepackets is identical in the whole set, the population and time evolution in the intermediate states is also identical. The propagation of the vibrational wavepackets over all allowed internuclear distances is monitored with a probe laser of variable intensity to detect the influence of high laser intensities on the molecular potential sensitive to the internuclear distance. The photoelectron signal for a probe laser intensity of $6 \cdot I_0$ is shown in Fig. 2b. The dynamic behavior has changed and the kinetic energy of the time of flight of the photoelectrons is slightly increased corresponding to a decrease of the photoelectron energy ($\approx 0.03 \text{ eV}$). In Fig. 3 the FFT of the cuts at TOFs corresponding to the inner and outer turning points of the wavepackets are shown.

At the inner turning point, we observe signals of the wavepacket in both the A- and Π -states. By increasing the probe laser intensity, the ratio of the signal in the FFT changes and the signal of the wavepacket in the A-state is becoming dominant compared to that in the Π -state. As mentioned above, there is no contribution of the A-state wavepacket at the attenuated probe laser intensity at the outer turning point. At an intermediate probe intensity of $2 \cdot I_0$, we observe an onset of the frequency of the A-wavepacket. This contribution increases rapidly with increasing probe laser intensity and becomes dominant for the highest intensity used ($10 \cdot I_0 \approx 10^{12} \text{ W/cm}^2$). At $6 \cdot I_0$ the signal heights of the wavepacket contributions in the FFT at the inner and outer turning point become comparable.

The increasing contribution of the frequency of the A-wavepacket with increasing probe laser intensity as compared to the frequency of the Π -wavepacket at the inner turning point might be attributed to the increased probability of two-photon absorption processes at high laser intensities. The electronic transition at the outer turning point out of the $A^1\Sigma_u^+$ -state with increasing probe laser intensities, however, cannot be explained by non-resonant two-photon ionization because this process would lead to a constant photoelectron energy for all allowed internuclear distances since the difference potential between the $A^1\Sigma_u^+$ -state and the ionic ground state is flat. An explanation of this behavior is possible in terms of light-induced potentials (see, e.g., Ref. [10] and references therein). Within this concept, the laser intensity affects the molecular potentials leading to adiabatic potentials. First theoretical calculations are performed using the split operator technique [26,27] and involving the $X^1\Sigma_g^+$ -, $A^1\Sigma_u^+$ - and $2^1\Pi_g$ -states. The transition matrix elements are supposed to be independent of the internuclear distance. The coupling to the ionic ground state is treated by perturbation theory, since the transition matrix element is about 10 times smaller than those in the neutral system [28].

Since the concept of difference potentials is capable to explain the photoelectron signal at attenuated laser intensities, i.e. where perturbation theory holds, we transferred this concept to higher intensities. For that purpose, we considered the calculated adiabatic dressed states for each laser intensity, denoted in the following as A^* and Π^* . At the limit of attenuated laser intensities, this adiabatic difference potential passes into the diabatic potential (Fig. 4) and the statements derived within the perturbation theory hold as discussed above. At a laser intensity of about 5×10^{11} W/cm² the adiabatic difference potential becomes almost flat over internuclear distances where the molecular wavepacket motion takes place (i.e. 3–5 Å). Within this context, there is no restriction of the transition between the A^* - and Π^* -state to a specific molecular configuration as in the diabatic limit and the transition probability is independent of the internuclear distance. At a laser intensity of $10 \cdot I_0$ the adiabatic difference potential increases with increasing internuclear distance resulting in a restriction of internuclear distances where transitions

from A^* to Π^* can take place. As explained, these adiabatic difference potentials give evidence to a change in the relative transition probability between the neutral adiabatic A^* - and Π^* -states in the sodium dimer. As a function of the probe laser intensity, the dependence on the internuclear distance of this probability changes.

The kinetic energy of the photoelectrons is determined by the difference potential between the Π^* -state and ionic ground state. According to the calculations, the monotonously increasing slope of this difference potential is similar for all laser intensities used. Therefore the relation between the kinetic energy and internuclear distance is given at high laser intensities as in the limit of low intensity (see Fig. 1). As a consequence, the different contribution of the dynamics in the $A^1\Sigma_u^+$ -state to the whole dynamics for increasing laser intensity is determined by the change of the difference potential between the adiabatic A^* - and Π^* -states. Therefore, the frequency of the A-wavepacket at a laser intensity of $6 \cdot I_0$ can be observed in the photoelectron spectrum independent of the internuclear coordinate since there is no limitation to a Franck–Condon window for a resonant ionization out of the A^* -state via the Π^* -state.

Calculating the photoelectron energy in our approach, we expect a decrease with increasing probe laser intensity of about 0.2 eV. This is more than the observed energetic shift of about 0.03 eV corresponding to the measured TOF of the photoelectrons. This might be an effect of a light-induced coupling of electronic states in the ionic system leading to a shift in the ionic ground-state potential [10], which was not included in our calculations. The Gaussian variation of the laser intensity across the spatial beam profile was also not taken into account. Full theoretical calculations to study the observed behavior are currently performed [29].

4. Summary

In summary, we have combined femtosecond pump–probe techniques and photoelectron spectroscopy in order to investigate the influence of intense laser fields on molecular potentials along the internuclear axis in Na₂ as a prototype molecule. By increasing the laser intensity, we observe electronic

transitions in intense laser fields at internuclear distances that are not allowed according to the Franck–Condon principle in the perturbation regime. The results demonstrate the possibility to generate molecular configurations that overcome the limitations that are usually given for electronic transitions due to the Franck–Condon principle. This concept is particularly important for femtochemistry and coherent control of chemical reactions [1–3].

Acknowledgements

The work was performed in the group of G. Gerber. We would like to thank G. Gerber, V. Engel and V. Seyfried for help and stimulating discussions. This work was supported by the Deutsche Forschungsgemeinschaft (DFG).

References

- [1] A.H. Zewail, *Femtochemistry*, vols. 1/2, World Scientific, Singapore, 1994.
- [2] J. Manz, L. Wöste, *Femtosecond Chemistry*, vols. I–III, VCH, Weinheim, 1995.
- [3] P. Gaspard, I. Burghardt, I. Prigogine, S.A. Rice, *Chemical Reactions and Their Control on the Femtosecond Time Scale*, XXth Solvay Conference on Chemistry, vol. 101, *Advances in Chemical Physics*, Wiley, New York, 1997.
- [4] L.J. Frasinski, K. Codling, P. Hatherly, J. Barr, I.N. Ross, W.T. Toner, *Phys. Rev. Lett.* 58 (1987) 2424.
- [5] H. Helm, M.J. Dyer, H. Bissantz, *Phys. Rev. Lett.* 67 (1991) 1234.
- [6] D.T. Strickland, Y. Beaudoin, P. Dietrich, P.B. Corkum, *Phys. Rev. Lett.* 68 (1992) 2755.
- [7] P. Dietrich, D.T. Strickland, M. Laberge, P.B. Corkum, *Phys. Rev. A* 47 (1993) 2305.
- [8] T. Seideman, M.Yu. Ivanov, P.B. Corkum, *Phys. Rev. Lett.* 75 (1995) 2819.
- [9] A. Zavriyev, P.H. Bucksbaum, J. Squier, F. Salane, *Phys. Rev. Lett.* 70 (1993) 1077.
- [10] M. Machholm, A. Suzor-Weiner, *J. Chem. Phys.* 105 (1996) 971.
- [11] A. Assion, M. Geisler, J. Helbing, V. Seyfried, T. Baumert, *Phys. Rev. A* 54 (1996) R4605.
- [12] T. Baumert, V. Engel, C. Meier, G. Gerber, *Chem. Phys. Lett.* 200 (1992) 488.
- [13] T. Baumert, G. Gerber, *Physica Scripta* T72 (1997) 53.
- [14] A. Assion, T. Baumert, J. Helbing, V. Seyfried, G. Gerber, in: P.F. Barbara, J.g. Fujimoto, W.H. Knox, W. Zinth (Eds.), *Springer Series in Chemical Physics, Ultrafast Phenomena X* 270, Springer, Berlin, 1996.
- [15] T. Baumert, M. Grosser, R. Thalweiser, G. Gerber, *Phys. Rev. Lett.* 67 (1991) 3753.
- [16] B.J. Greenblatt, M.T. Zanni, D.M. Neumark, *Chem. Phys. Lett.* 258 (1996) 523.
- [17] D.R. Cyr, C.C. Hayden, *J. Chem. Phys.* 104 (1996) 771.
- [18] P. Ludowise, M. Blackwell, Y. Chen, *Chem. Phys. Lett.* 258 (1996) 530.
- [19] V. Stert, W. Radloff, C.P. Schulz, I.V. Hertel, *Eur. Phys. J. D* 5 (1999) 97.
- [20] V. Blanchet, A. Stolow, *J. Chem. Phys.* 108 (1998) 4371.
- [21] T. Baumert, J. Helbing, G. Gerber, *Coherent Control with Femtosecond Laser Pulses*, vol. 101, *Advances in Chemical Physics*, Wiley, New York, 1997, pp. 47–77. See Ref. 3.
- [22] P. Kruit, F.H. Read, *J. Phys. E: Sci. Instrum.* 16 (1983) 313.
- [23] T. Baumert, B. Bühler, M. Grosser, R. Thalweiser, V. Weiss, E. Wiedenmann, G. Gerber, *J. Phys. Chem.* 95 (1991) 8103.
- [24] R.S. Mulliken, *J. Chem. Phys.* 55 (1971) 309.
- [25] T. Baumert, G. Gerber, *Isr. J. Chem.* 34 (1994) 103.
- [26] J.A. Fleck Jr., J.R. Morris, M.D. Feit, *Appl. Phys.* 10 (1976) 129.
- [27] A. Giusti-Suzor, X. He, O. Atabek, F.H. Mies, *Phys. Rev. Lett.* 64 (1990) 515.
- [28] C. Meier, V. Engel, *Phys. Rev. Lett.* 73 (1994) 3207.
- [29] V. Engel, S. Meyer, private communication.